Macroporous Gels of Poly(*N*,*N*-dimethylacrylamide) Obtained in the Lamellar System AOT/Water

I. E. Pacios,*,† A. Horta,‡ and C. S. Renamayor*,§

Departamento CC. y TT. Fisicoquímicas, Facultad de Ciencias, UNED, P°/Senda del Rey 9, 28040 Madrid, Spain

Received February 4, 2004; Revised Manuscript Received March 31, 2004

ABSTRACT: *N*,*N*-Dimethylacrylamide and *N*,*N*′-methylenebis(acrylamide) are copolymerized in the lyotropic AOT/water medium to yield several types of macroporous hydrogels. These gels are formed in two different macroscopic phases of the reacting system. The morphology of the gels, once isolated, is widely different depending on the macroscopic phase in which they were formed. Inside each phase, the polymerization induces an additional microscopic phase separation, with the result of deswelling of the original lamellar AOT/water structure. The morphology of the isolated gels is not a copy of this original nanostructure, instead, it has features whose length scales are larger than those of the starting phases. More complex morphological patterns develop in the presence of surfactant, as a result of the phase separation process. The type of morphology appears to be correlated with the proportion of water contained in the macroscopic phases. The swelling of the isolated gels in water does not follow the increase with chain length between cross-links predicted by network theory, probably because of the contribution from the macropores.

Introduction

The control of the structure of hydrogels represents an attractive subject of research, since applications such as chromatography, ultrafiltration, or catalysis require materials with controlled porous diameters. More recently, another application has been developed: tissue engineering. For this purpose, larger interconnected pores (macropores) are required, to allow the cellular invasion of the material (the minimum size required would be 10 μm). Macroporous hydrogels, also called hydrogel sponges, have been proposed to ensure a good adhesion between prosthetic implants and biological tissues.[1]

Practically, all industrially applied porous substances have two aspects in common: the pores are spatially disordered, and the pore geometries are characterized by broad size distributions.[2] For these reasons, there is an increasing demand to develop structurally well-defined porous systems. The lyotropic liquid-crystalline (LLC) phases, because of their characteristic long-range order, have been proposed[3] as a smart polymerization medium to produce pore controlled networks using just standard monomers.

In recent years, these type of studies have achieved great attention,[4,5] but only in a few cases is the parent structure maintained after polymerization.[6,7] Usually, the final hydrogel has a structure dramatically different from that of the initial system, because monomer consumption on one hand, and polymer formation on the other, strongly influence the morphology obtained. The polymer chains tend to coil and do not easily adapt to confined geometries,[8] but even when the template of the original structure is not obtained, a new interesting morphology usually appears, and the studies reveal that the generated morphology depends on the type of monomer and on the mesophase structure.[9]

Polymerization-induced phase separation is a method to prepare high porous thermoset networks. In this technique, additives in the initially homogeneous feed mixture segregate during polymerization, producing well-controlled porous materials;[10] these additives are usually polymer thermoplastics or solvents. More recently, the technique has been extended to prepare porous hydrogels; i.e., macroporous acrylamide hydrogels have been synthesized by the addition of hydrophilic polymers[11] and nonsolvents[12] to the monomer mixtures.

In previous work, we have studied mixtures of the linear polymer poly(*N*,*N*-dimethylacrylamide) (PDMAA), with the lamellar surfactant system formed by bis(2-ethylhexyl) sulfosuccinate sodium salt, namely, Aerosol OT (AOT), and water,[13,14] and also the in situ[15,16] linear polymerization of the monomer *N*,*N*-dimethylacrylamide (DMAA) in the same lamellar system AOT/water. In this system, the linear polymer, whether prepared separately and then mixed with the surfactant, or prepared by in situ polymerization of the monomer dissolved in the surfactant, segregates from the lamellae and forms an isotropic microphase, which does not macroscopically separate. This polymer-rich phase modifies the structure of the lamellar mesophase and deswells it.[17]

Here, the morphosynthesis of porous cross-linked poly(*N*,*N*-dimethylacrylamide) in the AOT/water system is described. We consider three points, which refer both to the structure of the mesophase used as template and to the structure and behavior of the hydrogels formed: (a) the modification induced in the lamellar structure of the mesophase by the cross-linking polymerization, as compared to that induced by the linear polymerization; (b) the different morphologies developed in the gels when they are formed in the AOT/water system, as compared to the conventional ones formed in pure water; (c) the different swelling capacity of these two types of hydrogels. For these purposes, the techniques of polarized light microscopy, scanning electron micros-

† E-mail: ipacios@ccia.uned.es.
‡ E-mail: arho@ccia.uned.es.
§ E-mail: csanchez@ccia.uned.es.

10.1021/ma049758j CCC: $27.50
Published on Web 05/14/2004

Table 1. Global Composition of the Samples

sample	H_2O (g) ± 0.001 (g)	DMAA (g) ± 0.0002 (g)	BA (g) ± 0.0001 (g)	AOT (g) ± 0.0001 (g)	S (g) ± 0.0001 (g)	AIBN (g) ± 0.0001 (g)
PB1	69.999	7.9134	0.0989	25.0883		0.0117
PB2	67.006	7.9188	0.0990	25.0109	0.0033	0.0113
PB3	67.173	3.2363	0.1247	25.0027		0.0118
G3.4	28.968	1.0139	0.0397			0.0053
G7.3	30.024	2.3816	0.0302			0.0045
G7.9	27.784	2.3787	0.0294			0.0043
G8.1	27.627	2.4488	0.0300			0.0042

copy (SEM), small-angle X-ray scattering (SAXS), and fluorescence emission spectroscopy were employed. The samples were characterized before and after polymerization and were also studied after removal of the surfactant.

Experimental Section

Materials. AOT and DMAA (99% purity) were purchased from Sigma and Aldrich, respectively, and *N*,*N*′-methylenebis-(acrylamide) (BA) (99.5% purity) was obtained from Fluka. All of them were used as received. AIBN (α,α′-azobis(isobutironitrile) was purchased from Fluka and was crystallized from methanol. Deionized water (Milli-Q) was used for the preparation of samples.

N-(2-aminoethyl)-5-(dimethylamino)naphthalene sulfonamide (S) was used as a fluorescent probe, the synthesis method and characterization were described elsewhere.[13,18,19]

Techniques. Small-Angle X-ray Scattering (SAXS). SAXS measurements were performed on a modular equipment.[20] A narrow slit was used before the sample to minimize the background scattering. The primary beam is narrow, the full width at half-maximum ($fwhm_{inst}$) is 0.001 $Å^{-1}$. The smallest achievable wave vector (**k**) is only ca. 0.05 $Å^{-1}$ by using this setup. The results are plotted by using $\mathbf{k} = (4\pi/\lambda)\sin\theta$, where $\lambda = 1.542$ Å and 2θ is the scattering angle. The samples were placed in a holder between cover films of polyimide and were observed at room temperature.

Optical Microscopy. A microscope (Nikon Labophot-2) provided with a Nikon camera (model F-601) and crossed polarizers was employed to determine the anisotropy of the samples. During these measurements the samples were placed between a glass slide and a coverslip

Scanning Electron Microscopy. After removing the template, the swollen hydrogels were dried by the critical-point technique, after a gradient exchange of water by acetone and subsequent exchange to supercritical CO_2, using a Balzers CPD 030 critical point dryer. Then, these samples were sputtered with Au, using a Balzers SCD 004 sputter coater, and finally characterized using a JEOL JSM 6400 scanning microscope.

Steady-State Fluorescence Spectroscopy. Fluorescence emission spectra were recorded on an Aminco-Bowman SLM 2. The emission spectra were corrected using the instrumental response at each wavelength. The excitation wavelength was set at 325 nm, the maximum in the absorption spectra of *N*-(2-aminoethyl)-5-(dimethylamino)naphthalene sulfonamide (S). Slits of 4 nm, both for emission and excitation, were used.

Sample Preparation and Analysis. Polymerization. Lyotropic solutions were prepared by mixing aqueous solutions of monomers and initiator with the proper amounts of AOT (see Table 1). Two samples with similar compositions, named PB1 and PB2, were prepared to examine reproducibility. PB2 contains also a little amount of the fluorescent probe (S). A third sample, PB3, with a lower DMAA concentration, was prepared to consider the effect of a different monomer/cross-linker ratio. In the three samples, the ratio AOT/water is kept always constant (0.015). To prepare the feeding mixture, the proper amount of AIBN, the comonomers (and the fluorescent probe in PB2) were dissolved in water, and then it was added the AOT, followed by stirring to homogenize the mixture. The samples were then let to equilibrate at 25 °C (at this stage, two phases are developed in samples PB1 and PB2). To polymerize, the mixtures were kept slightly above 60 °C for 1 day. After this, they were allowed to cool and stay at 25 °C for several days. The total mass is about 100 g; this allows obtaining enough amount of sample to study and characterize the macroscopic phases that appear after polymerization.

Table 1 also reports the composition of four reference hydrogels that were synthesized in an homogeneous medium (water). Their polymerization was carried out at 60 °C in an oven for 24 h. Samples were named G8.1, G7.9, G7.3, and G3.4, where the number refers to the percentage of monomer (w/w) in the feed mixture.

Composition. After polymerization, the composition of the different macroscopic phases that appear was analyzed, by using independent methods for each component. The AOT has been determined using a standard spectrophotometric method (ISO 7875) for the determination of anionic surfactants. The water content was obtained by drying in an oven a known amount of a given phase, and subtracting this weight from the initial one. The hydrogels obtained in the several phases were washed with water several times to eliminate the remaining monomer and AOT, and the polymer content was then determined after drying.

Swelling. To measure swelling, disk like xerogel samples were used, and the swelling was determined gravimetrically. Each xerogel sample was immersed in deionized water, and after a certain time the hydrogel surface was gently dried with soft tissue and weighed.

Results and Discussion

Macroscopic Phases. Before polymerization, samples PB1 and PB2 present two phases. As also found in previous studies[15,16] related with the polymerization of DMAA without cross-linker in the lyotropic AOT/water medium, the upper phase is clear and isotropic and the bottom phase is turbid and lamellar. Along with polymerization, the macroscopic phase separation progresses, as also occurs in the un-cross-linked system, this being indicative that effective cross-linking does not take place at the beginning of the synthesis but after a certain conversion is attained.[21] When polymerization finishes and 25 °C is recovered, we can observe, from the first day of equilibration, four phases in sample PB2, while only three phases can be observed for sample PB1, even after waiting more than 1 month for equilibration.

Among the different phases finally obtained after polymerization in samples PB1 and PB2, there are two that we can consider the most important ones: the bottom (B) and the next to the bottom (C). Their combined volume is 95% (in sample PB1) and 81% (in sample PB2) of the total volume. Both are turbid and very viscous, in fact the C phase keeps its shape since it contains a consistent gel. The upper phases (U) are quantitatively less important, they are quite fluid, giving no evidence of gel presence. After the phases are isolated to perform their characterization, the less dense phase in sample PB2 seems to be in pseudoequilibrium, since it splits into two macroscopic phases, one clear (the upper) and the other turbid.

The sample PB3, with a smaller monomer content, presents only one phase at 25 °C and remains monopha-

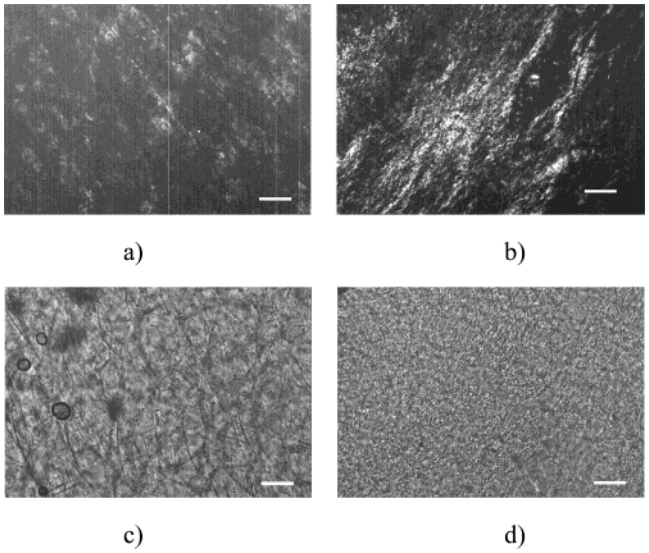

Figure 1. Micrographs from phases belonging to sample PB1. With crossed polarizers: (a) phase C; (b) phase B. Without crossed polarizers: (c) phase C; (d) phase B. Bar: 100 μm.

Table 2. Composition of the More Important Macroscopic Phases of Samples PB1, PB2, and PB3, after Polymerization

sample	phase	% vol	% AOT	% H_2O	% gel
PB1	C	67	23	64.08 ± 0.07	8.09
PB2	C	53	19 ± 6	65.14 ± 0.04	7.52
PB1	B	28	28 ± 4	61.42 ± 0.07	4.90
PB2	B	28	21 ± 6	55.52 ± 0.05	3.8
PB3	B	82	27 ± 1	70.40 ± 0.01	1.88

sic when heated to 64 °C; nevertheless, when polymerization advances at this temperature, the sample separates into two phases. Finally, when the polymerized sample is cooled back to 25 °C, a third phase appears. The bottom phase (B) is turbid and occupies most of the final volume (82%), the upper phases (U1 and U2) have much smaller relative volumes (6 and 12%, respectively) than the B phase and do not contain a significant amount of gel, so they are not very important for the purpose of this work.

After the equilibration period, the different phases were separated to perform the characterization. Table 2 summarizes the global composition of B and C phases. Both show a similar composition in samples PB1 and PB2, which ensures the reproducibility of the experiment. After comparing the compositions of the B and C phases, we can conclude that the polymer gel is generated preferentially in the C phase.

Mesophase Structure. The turbidity of the C and B phases suggests that there is phase separation in them, and their respective micrographs without crossed polarizers (see, e.g., Figure 1, parts c and d) evidence a clear phase-separated pattern. So, the turbidity can be related to the presence of two domains with different refractive indexes.[13] On the other hand, optical micrographs obtained with crossed polarizers show the typical marbled lamellar texture (see, e.g., Figure 1, parts a and b); this indicates that C and B contain, at least, one lamellar phase.

In the small angle region of X-ray scattering (SAXS) we obtain information about long range order in the samples. In a lyotropic lamellar system the Bragg peaks have a relative position 1:2:3:4..., and the intensity of the first-order peak is usually higher than the others. Figure 2 depicts the SAXS diffractograms of C and B phases from sample PB1. These patterns were tested for 10 months after the phases were separated, to check that they did not change. Both phases show a broad hump for wave vector between 0.1 and 0.5 Å^{-1}, which is characteristic of the AOT−water system.[22] In the bottom phase we also detect two peaks, at relative positions 1:2.02, in accordance with a lamellar structure, and the intensity of both peaks are similar. However, in the C phase there is only one peak, located at about 0.24 Å^{-1}. This is typical of the lamellar phase in the AOT/water system,[23] where the intensity ratio between the first and the second-order peaks depends on composition and even the first-order peak can disappear. This same behavior was also found with the linear polymer.[14] The pattern of the B phase from sample PB3 contains the same broad hump and three peaks, with relative positions (1:1.99:2.98) that agree also with the lamellar structure. Additionally, the intensity of the first peak is lower than that of the second one.

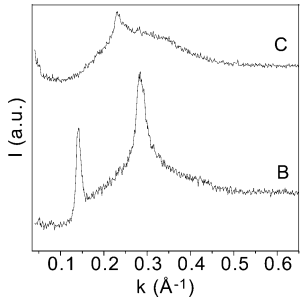

Figure 2. SAXS diffractograms for phases C and B of sample PB1.

So, the information from X-ray scattering reinforces that from optical microscopy, and from both types of results, we can conclude that the phases B and C of all three samples (PB1, PB2, PB3) are microheterogeneous and contain a lamellar structure in one of the microphases. We can try to get more information about the lamellar microphases using fluorescence, since this technique is useful to study microheterogeneous systems.

The emission spectrum of fluorescent probe S is sensitive to the polarity of the environment,[24] the ratio of intensity at 497 and 539 nm decreases strongly when the polarity of the medium increases. In a previous work,[13] we deduced that in the lamellar AOT/water system, the probe is located in the interfacial region of the bilayer, close to the AOT hydrophilic groups, with a ratio $I_{497}/I_{539} = 0.89 \pm 0.03$, Fluorescence spectra of C and B phases from sample PB2 have ratios $I_{497}/I_{539} = 0.91$ and 0.90, respectively. These values are similar to that of the probe in the binary system; consequently, we can conclude that the polymer does not affect the polarity of the probe environment, and consequently, the polymer gel is not near the bilayers, in agreement with a phase-separated model.

The above results (optical microscopy, SAXS, and fluorescence experiments), agree with the previous study about linear polymerization of DMAA without cross-linker in the AOT/water system;[15] thus, we can conclude that the polymerization induces a microscopic phase separation (secondary process) within the macroscopic phases (primary process): the polymer segregates from the lamellae and forms an isotropic polymer-rich microphase, which coexists with a surfactant-rich lamellar phase (Scheme 1).

Scheme 1. Proposed Model for the Result of the Phase Separation Secondary Process that Yields a Surfactant-Rich Lamellar Microphase and a Polymer-Rich Isotropic Microphase

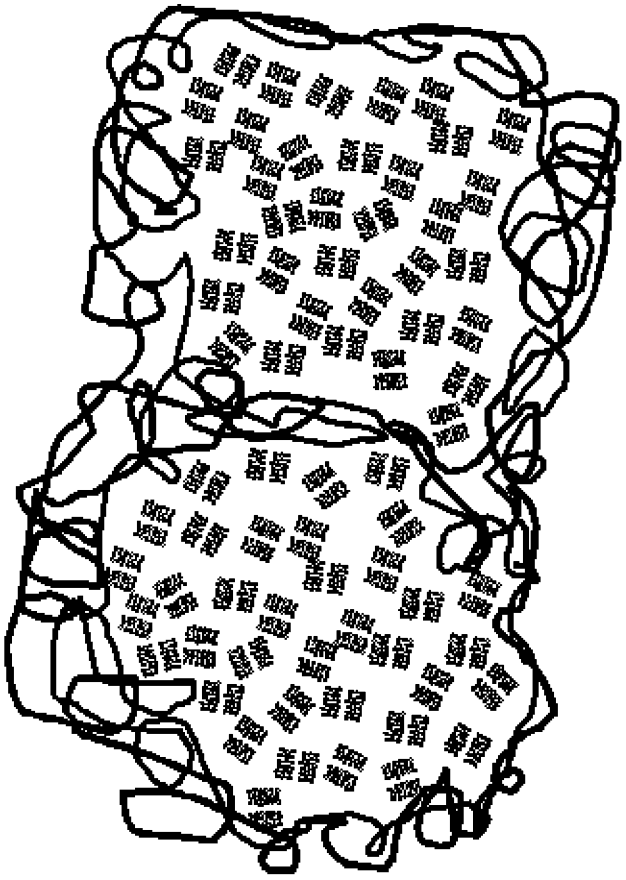

The structure of the liquid crystalline mesophase is modified by the gel formation (the in situ cross-linking polymerization) in much the same way as it is modified by the linear polymerization. The microphase separation induced by polymerization is accompanied by deswelling of the lamellar structure, because the polymer forms its isotropic microphase by taking some water from the AOT/water. This deswelling of the lamellar structure is detected by a shortening of the long period spacing of such lamellae. The location of the SAXS diffraction peaks (Figure 2) allows determining such long period spacing (d) of the lamellar structure. In a bicomponent system (sufactant/water) the long period can be determined using a simple dilution law $1/d = (1/d_i)\phi_i$ where d_i is the layer thickness and ϕ_i is the volume fraction of the component i (in our case AOT or water). For these kind of systems, where there is also a polymer-rich microphase, coexisting with the lamellar one, that does not separate macroscopically from it, we have calculated the deswelling of the lamellae, as a function of the amount of polymer present.[13] Assuming equilibrium between the lamellar and isotropic microphases, we arrived at the general dilution law, encompassing both the influence of surfactant and polymer concentrations on the lamellar spacing, d. In the case of AOT and PDMAA, it reads[15]

$$\frac{1}{d_{II}} = \frac{1}{d_{AOT}}(\phi_{AOT} + K\phi_{PDMAA}) \qquad (1)$$

where K is the coefficient which represents the partition of water between the two microphases in equilibrium. The value of K was determined from mixtures with the linear polymer PDMAA previously synthesized in pure water, with the result $K = 1.8$[15] and $d_{AOT} = 19.6$ Å.[25]

Table 3. Long Period Spacing of the Lamellar Structure AOT/Water[a]

sample	phase	d (Å)	d_{II} (Å)
PB1	C	53.9	52
PB2	C	50.9	59
PB1	B	44.6	53
PB2	B	46.5	60
PB3	B	64.2	68

[a] Key: d, experimental value; d_{II}, value calculated assuming equilibrium deswelling of lamellae by the polymer (eq 1), with K fitted to results from mixtures of AOT/water with linear polymers), for phases C and B from samples PB1 and PB2 and for phase B from sample PB3

Table 3 presents the experimental data of d from SAXS measurements and the values calculated with eq 1. Theoretical values are higher than the experimental ones; that is, the real lamellar spacing in these gel samples is shorter than that predicted by the dilution law in eq 1. This dilution law takes into account the deswelling of the lamellar structure exerted by the polymer, and the value of the partition coefficient was determined with linear polymers. The shorter experimental spacings found here could be described by a higher value of the partition coefficient, K, which means more water in the gel and less water in the lamellae. Hence, an even stronger deswelling exerted by the gels in the in situ cross-linking polymerization as compared to that exented by the linear polymer obtained in pure water when mixed with AOT/water. However, we cannot disregard the inaccuracy in the determination of phases composition, since any AOT or polymer not properly recovered would increase the spacing predicted with eq 1.

The determination of phases composition has here a great inaccuracy because of the difficulty in handling the gels. The composition of phases could be determined with a much higher accuracy in the case of the linear polymers obtained by in situ polymerization.[15] Nevertheless, with linear polymers, a similar effect of a stronger deswelling was observed,[15] so it seems a real phenomenon and not the result of experimental error. Both in the present cross-linked gels and in previous linear polymers, the greater deswelling occurs in phase B. The lamellar structures of phases B and C are formed at different stages of the polymerization. Phase C becomes lamellar when cooling after the in situ polymerization, while phase B is lamellar from the beginning. So, the lamellae in phase C are formed by a process more akin to the mixing of AOT/water with a polymer already formed, which was the basis for the value of coefficient K used to calculate d_{II} in eq 1. When the polymer is formed in the already lamellar phase B, the result of polymer segregation is a stronger deswelling of the lamellae (corresponding to a higher value of K). Equation 1 holds for equilibrium, and the need of a different value of the partition coefficient may reflect metastability in the system (in fact, the isotropic and lamellar microphases do not separate macroscopically).

Hydrogel Morphology. In this section, we analyze the morphology of the purified hydrogels, in relation to the process of their formation. In a simplified process of hydrogel formation by free radical copolymerization, linear polymers with branching units are first formed

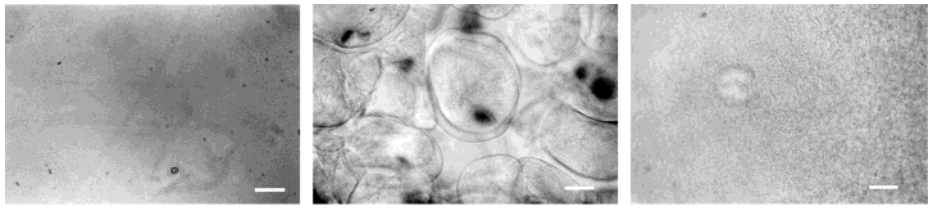

a) b) c)

Figure 3. Micrographs from swelled hydrogels: (a) gel G7.3 (obtained in pure water); (b) gel from phase C of sample PB2 (obtained in the AOT/water medium); (c) gel from phase B of the same sample PB2. Bar: 100 μm.

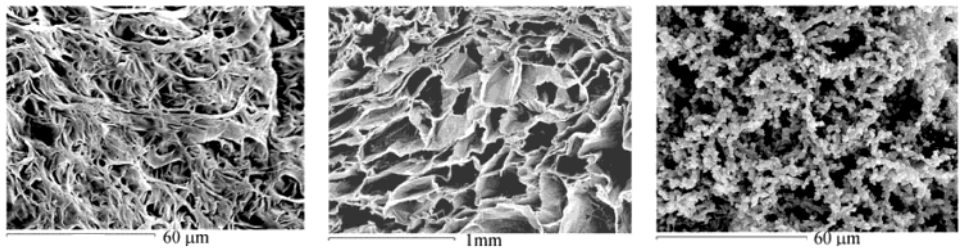

a) b) c)

Figure 4. Scanning electron microscopy pictures of gels: (a) gel G7.3 (obtained in pure water); (b) gel from phase C of sample PB2 (obtained in the AOT/water medium); (c) gel from phase B of the same sample PB2.

in the fast propagation step to form "primary molecules",[26] which are later cross-linked to form a three-dimensional network. One of the most interesting properties of an hydrogel is the porosity, which is determined by the extent of interpenetration of polymer chains within the gel network after the "gel point".

When comparing the hydrogels that have been polymerized in the presence of AOT with those synthesized in water, we observe that their morphologies are rather different. Optical microscopy (OM) in conjunction with scanning electron microscopy (SEM) allows the study of such morphologies. In Figures 3 (OM) and 4 (SEM) we compare the micrographs of a sample gel obtained in pure water (Figures 3a and 4a) with those of a sample gel obtained in the AOT/water media, in phases C (Figures 3b and 4b) and B (Figures 3c and 4c). OM does not reveal any characteristic texture for the PDMAA gel synthesized in water (Figure 3a), and SEM reveals a dense structure for this gel (Figure 4a). On the other hand, gels obtained in the AOT/water medium are porous and show two different morphologies. One looks like a foam (Figures 3b and 4b), and we can appreciate a layerlike macroporous morphology at the millimeter scale. The other (Figures 3c and 4c) is formed by primarily small polymer spheres that are joint to form a rather continuous mesoporous network (open pores); the question is why they are so different.

One could analyze this result in terms of a different length of the "primary polymer chains" due to a different composition of the medium where they are formed,[27] but in a previous work, where we synthesized linear PDMAA in the AOT/water medium, we have observed that the molecular weight in all phases is the same, and also similar to that obtained for a polymer synthesized in pure water,[15] so this is not the likely origin of the different morphology found. Another explanation must be sought.

In samples PB1 and PB2 before polymerization, the system is located in a biphasic (isotropic−lamellar) region. During polymerization, the appearance of polymer and the consumption of monomer produce the displacement of the biphasic region to lower AOT concentrations; therefore the isotropic phase splits into two: the upper being still isotropic and the phase which we call C, having a lamellar structure. As a result, a lamellar phase is generated during polymerization.[16] The origin of gel in phase B is rather different; it is generated in the bottom phase, which is lamellar from the beginning (in the three samples PB1, PB2, and PB3). During polymerization, the polymer segregates from the already existing lamellae, and competes with the surfactant for the water, so, as the polymer grows, the lamellae shrink. Despite this, the morphology found in the gels does not seem to be related with the original order in the two phases, as we shall see.

It has been proposed that the formation of unusually large pores in this kind of systems is consequence of the competition between the spinodal decomposition of polymer mixture and the gelling process, which prevents the macroscopic separation.[28] The architecture is a result of the demixing[9] and the gel morphology depends on the step in which gelification takes place.[29] If the system is very viscous, the coarsening of decomposition is stopped in the first steps. This occurs when the concentration of water is low; nevertheless, when the viscosity is not too high, the coarsening evolves to the last steps.

By looking at Table 2, we can check that the gels from samples with higher water content present macroporous morphology (see Figure 4b). This occurs in the case of phase B from sample PB3 and phase C from samples PB2 and PB1, while for phase B from sample PB2, which is the phase with lowest water content, the gel formed consists of open pores (Figure 4c). For an intermediate concentration of water (phase B from sample PB1), we can observe a mixture of both morphologies; the coarsening of the primary polymer spheres gives sheetlike structures that conform the macropores (Figure 5).

We can conclude that the morphology is not a copy of the original nanostructure of the AOT/water mesophase. The gel morphology shows features with length scales

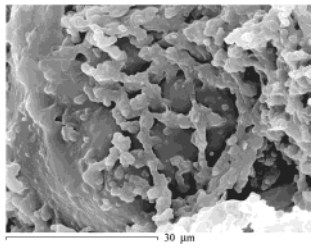

Figure 5. Scanning electron microscopy picture of gel from phase B of sample PB1.

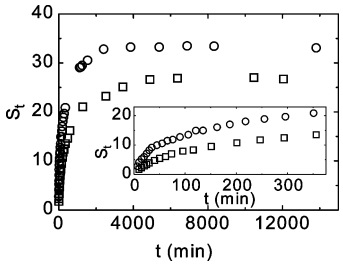

Figure 6. Swelling vs time for a hydrogel obtained in the AOT/water medium (from phase C of sample PB1) (○) and for a hydrogel obtained in pure water (G7.3) (□).

much larger than the characteristic length of the template, since they occur at the mesoscopic level (micrometers to millimeters). More sophisticated hierarchical and regular patterns appear when the gels come from the segregation process occurring in the presence of surfactant. Furthermore, the wide differences between the type of morphology found in each macroscopic phase, are due to the larger restriction to phase coarsening imposed by the viscous AOT/water system (the restriction is higher in the phases with lower water content).

Swelling. The swelling, S_t, is defined as

$$S_t = \frac{M_t}{m_0} \tag{2}$$

where M_t is the mass of water absorbed at time t, and m_0 is the mass of the dry gel. S_t increases with time to reach a plateau, usually named the maximum swelling degree or swelling at equilibrium, S_e. Figure 6 shows the swelling-time curves for the hydrogel C from PB1 and for the hydrogel G7.3 synthesized in water. The swelling rate in the first case is greater than in the second one, and the equilibrium is also reached earlier. This could be related to the gel morphology, since the macropores increase the contact area between the polymer network and the bulk water.

To find out the transport mechanism, data from the initial swelling were fitted to the following exponential equation:[30]

$$M_t/M_\infty = kt^n \tag{3}$$

Here M_∞ is the mass of water absorbed at equilibrium, k is a characteristic constant of the hydrogel, and n is an exponent related with the transport mode. n and k can be calculated from the slope and intercept of the graphs $\log(M_t/M_\infty)$ vs $\log t$, for values of $M_t/M_\infty < 0.6$. n equal 0.5 indicates Fickian diffusion, a value $0.5 < n < 1$ indicates non-Fickian or anomalous transport, and $n = 1$ implies case II (relaxation-controlled transport). In the samples studied here, $n = 0.5$ in both cases, whether it be the gel formed in the AOT/water system or in pure water. This $n = 0.5$ would suggest a Fickian mechanism for the diffusion process, which means that in both cases the network chains are well relaxed. According to the kinetic results, the diffusion coefficient should be larger for the gel synthesized in AOT/water than for the gel synthesized in pure water, but we cannot extract precise values for such coefficient (from k en eq 3), because the geometry of the samples is not exactly a disk but rather a short cylinder

Another important parameter for a polymer network is the molecular weight between effective cross-links (M_c), which describes the average molecular weight of the polymer chains between consecutive junctions points. These junctions may be chemical cross-links, physical entanglements, crystalline regions, or even polymer complexes,[31] but here only the first two types are expected. M_c is calculated from eq 4[32]

$$\ln(1-\phi_2) + \phi_2 + \chi\phi_2^{\,2} = -\frac{\rho_2}{M_c} V_1 \left(\phi_2^{\,1/3}\phi_{2r}^{\,2/3} - \frac{\phi_2}{2}\right) \tag{4}$$

where ϕ_2 is the polymer volume fraction in the swollen gel at equilibrium, ϕ_{2r} is the polymer volume fraction in the reference state at cross-linking, V_1 is the solvent molar volume, and ρ_2 is the xerogel density (approximately equal to that of the linear polymer: 1.06 g/cm^3). χ is the Flory−Huggins polymer−solvent interaction parameter, which can be obtained from

$$\chi = 0.5 - \rho_2^{\,2} V_1 A_2 \tag{5}$$

where A_2 is the second virial coefficient of PDMAA in water (3.4×10^{-4} mol m^3 kg^{-2}).[33]

The reference state is usually identified with the state of the relaxed network at the synthesis. In the case of gels synthesized in water, ϕ_{2r} is just the volume fraction of comonomers in the feed mixture, but when the gel is synthesized in the AOT/water system, ϕ_{2r} should be redefined, because there are two microphases: the surfactant-rich phase and the polymer-rich phase. If the network infinite structure is formed by cross-linking primary chains already formed, then such cross-linking takes place in the segregated polymer-rich microphase and thus, the volume fraction of the reference state should be defined in such a phase. This means defining ϕ_{2r} as

$$\phi_{2r} = \frac{v_2}{v_2 + v_1^{\,P}} \tag{6}$$

where v_2 is the polymer volume and $v_1^{\,P}$ is the water volume in the polymer-rich phase. This water volume cannot be determined directly in this isotropic phase, but can be calculated from total water and the water volume in the other phase (surfactant-rich), which is lamellar and allows the determination of its water contents from the thickness of the water layers between lamellae, as reported in previous work.[15]

The effective cross-links mole fraction, F_c, is calculated assuming tetrafunctional knots as

$$F_c = \frac{M_o}{2M_c + M_o} \tag{7}$$

where M_o is the monomer molecular weight (DMAA).

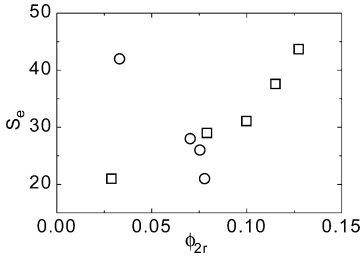

Figure 7. Swelling at equilibrium, S_e, as a function of the gel volume fraction in the reference state at cross-linking, ϕ_{2r}: (○) hydrogels synthesized in water and (□) hydrogels synthesized in the AOT/water medium.

Table 4. Polymer Content, in Weight, for the Different Samples Here Studied, % Gel, Gel Volume Fraction in the Cross-Linking Reference State, ϕ_{2r}, Calculated with the Water Volume in the Segregated Polymer-Rich Microphase, ϕ'_{2r}, Calculated with All the Water Volume, Swelling at Equilibrium of the Hydrogel, S_e, Molecular Weight between Cross-Links, M_c (from Eq 4), and Mole Fraction of Effective Cross-Links, F_c (from Eq 7), for the Hydrogels Studied in This Work

sample	phase	% gel	ϕ_{2r}	ϕ'_{2r}	S_e	M_c	$F_c \times 10^3$
G8.1		8.1	0.078	0.078	21.3	1.9×10^4	2.55
G7.9		7.9	0.075	0.075	26.5	3.7×10^4	1.34
G7.3		7.3	0.070	0.070	28.5	4.3×10^4	1.15
G3.4		3.4	0.033	0.033	42	4.9×10^4	1.00
PB1	C	8.09	0.13	0.11	43.7	1.8×10^5	0.27
PB2	C	7.52	0.12	0.098	37.6	1.2×10^5	0.42
PB1	B	4.90	0.10	0.070	31.1	6.8×10^4	0.73
PB2	B	3.8	0.079	0.060	29.0	4.7×10^4	1.1
PB3	B	1.88	0.029	0.025	21	6.0×10^3	8.1

Table 4 shows the characterization parameters (ϕ_{2r}, S_e, M_c, and F_c) for hydrogels studied in this work. The hydrogel swelling at equilibrium is a function of cross-linker ratio, hydrophilicity, and elasticity of the polymer network.[34]

The maximum swelling depends on the feed mixture composition, as it is well-known that, for hydrogels synthesized in an homogeneous medium, the maximum swelling becomes lower when the comonomers content increases. This is the behavior observed here for the gels synthesized in pure water, namely: G8.1, G7.9, G7.3, and G3.4 gels (Figure 7). Their equilibrium swelling, S_e, decreases parallel to the increase of comonomers in the initial mixture (as measured by ϕ_{2r}) or to the increase in percentage of gel formed (% gel). As the swelling degree of these gels formed in pure water gets greater, the calculated molecular weight between effective cross points, M_c, is higher and the effective cross-link mole fraction, F_c, is lower, all as expected from their initial mixture composition.[35]

For the gels synthesized in the presence of AOT (namely: PB1, PB2, and PB3), the trend with initial mixture composition is different, however. We can see in Table 4 that, in the gels formed in phases C and B, the swelling, S_e, is greater for sample PB1 than for sample PB2. The calculated values for the molecular weight between effective cross-links and for the effective cross-link mole fraction deduced for these two samples are still in accordance with expectations from elasticity theory, because M_c is higher and F_c is lower in the gels from sample PB1 than in the gels from sample PB2. However, the correlation with the initial comonomer content (ϕ_{2r}), or with the percent of gel formed (% gel), is opposite to that expected. Surprisingly, the equilibrium swelling of the gels synthesized in the presence of AOT increases as the amount of monomer in the initial mixture, ϕ_{2r}, is greater. This is seen by comparing again the gels of PB1 with those of PB2 in a given phase but, even more, considering the gels from both phases, B and C, of these two samples, together with the gel of sample PB3. All five gels (C and B, from PB1 and PB2, plus PB3) describe a collective trend: S_e increases as ϕ_{2r} and %gel increase, which is contrary to what is expected from the known behavior for gels formed in solvents without surfactant.

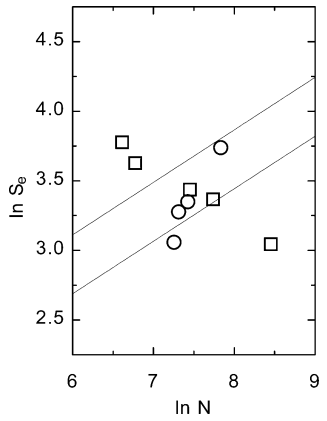

Figure 8. Log of the swelling at equilibrium (ln S_e) vs log of the length of the chains between cross-links in the gel (ln N): (○) hydrogels synthesized in water and (□) hydrogels synthesized in the AOT/water medium.

This paradox is not attributable to our redefinition of ϕ_{2r} as volume fraction in the polymer-rich phase, eq 3. Let us return to the usual definition of ϕ_{2r} as volume fraction in the whole reacting system. Then, in place of v_1^P, in eq 3 we use all the water volume, v_1, obtaining the values of column ϕ'_{2r} in Table 4. We can see that the paradoxical increase of equilibrium swelling with ϕ_{2r} is still maintained.

To attempt an explanation we must consider that an increase of the BA concentration produces the formation of more covalent cross-links, and an increase in the total monomer concentration intensify the entanglement formation. From the quantitative point of view this can be analyzed in terms of the scaling law between the length of the chain between cross-links (N) and the equilibrium swelling degree, proposed by Bromberg et al..[35] For PDMAA cross-linked with BA, they report a slope of the plot of ln S_e vs ln N equal to 0.377, and similar values have been obtained for other hydrogels,[36] although the theoretical value predicted by the Flory–Huggins theory for good solvents[26] is 0.6. N can be estimated by the following equation:

$$N \approx [a^6 c_{xl}(c_m + c_{xl})]^{-1} \tag{8}$$

Here c_{xl} and c_m are the initial molar concentration of monomer and cross-linker and $a^6 = 10 v_{xl} v_m$, $v_{xl} = 0.128$ M^{-1} and $v_m = 0.103$ M^{-1} being the molar volumes of BA and DMAA, respectively.

Figure 8 depicts ln S_e vs ln N for samples here studied. In this graph, the two solid lines limit the region where the experimental values obtained by Bromberg et al are located. In the same figure, the circles correspond to the hydrogels synthesized in water in this work and squares refer to samples obtained in the presence of AOT.

c_M and c_{xl} are well-known for hydrogels synthesized in water, whereas for the others some assumptions must be made: (i) The concentration of monomers in each

phase is calculated from the final gel concentration in each phase and assuming a 100% yield. (ii) In each phase, the monomer is homogeneously distributed in the water domain. (iii) The proportion between cross-linker and monomer is the same than in the feed mixture. We can appreciate in this graph that circles fit reasonably well to the zone delimited by the solid lines, although the gels formed in the presence of AOT define the opposite tendency. The point now is to find an explanation for the anomalous behavior. With this purpose we can argue that hydrogels obtained in the AOT/water system are porous, and their porosity comes from a phase separation process that is kinetically controlled. So, changing the monomer concentration can produce two different effects: to generate pores having a different size distribution and to modify the effective cross-linking. Swelling is the result of network dilation plus pore filling. Only network dilation is controlled by the chain length between cross-links. The contribution from pore filling is not deduced from the present experiments, and a correlation between swelling and the type of morphology of the gel is not found either. So, the question remains open. However, it is remarkable that the swelling shows such a nice correlation with the monomer or gel concentrations, the problem being that the correlation is opposite to that of gels obtained by conventional means.

Conclusions

The cross-linking polymerization of PDMAA in the medium AOT/water yields hydrogels having different morphologies, ranging from layerlike macroporous gels (at the millimeter scale) to granular continuous mesoporous networks (open pores). During and after polymerization, there is a macroscopic phase separation process, and simultaneous to it, the macroscopic phases are microheterogeneous, because the polymer formed segregates from the lamellar structure. The morphology of the gels is not a copy of the lamellar nanostructure of the mesophase. The obtained gels present morphologies whose features appear on length scales larger than those of the starting phases, and are more sophisticated because they come from a phase separation process. Phase coarsening restricted by the high viscosity of AOT could be the origin of the different morphology in each macroscopic phase, as there is a correlation with the amount of water diluting the phase.

The cross-linking polymerization evolves similarly to the linear polymerization without cross-linker, which suggests that the effective cross-links are formed at the last steps of the synthesis, as expected in a gelification process. Because of the segregation of the polymer from the lamellar structure, the network should be formed in equilibrium with only a fraction of the total water. Swelling of the gels obtained from the AOT medium decreases with increasing chain length between cross-links (this being determined in the same way as for gels synthesized in water). This dependence is contrary to conventional network theory and could be due to the participation of the macroporous morphology on total swelling.

Acknowledgment. Financial support from CICYT (Spain) under Grant BQU2000-0251 is gratefully acknowledged. Scanning microscopy measurements were made in the JEOL JSM 6400 microscope located in the Center of Electron Microscopy "Luis Bru" (Madrid). We gratefully acknowledge Profs. Olli Ikkala (Department of Engineering Physics and Mathematics, Helsinki University of Technology, Finland) and Mika Torkkeli (Department of Physical Sciences, University of Helsinki, Finland) for the SAXS determinations and for their hospitality and helpful advice with I.E.P. during her visit. Finally, we specially thank Inés F. Piérola for her helpful comments.

References and Notes

(1) Chirila, T. V.; Constable, I. J.; Crawford, G. J.; Vijayasekaran, S.; Thompson, D. E.; Chen, Y. C.; Fletcher, W. A.; Griffin, B. J. *Biomaterials* **1993**, *14*, 26−38.
(2) Beginn, U. *Adv. Mater.* **1998**, *10*, 1391−1394.
(3) Hentze, H. P.; Antonietti, M. *Curr. Opin. Solid State Mater. Sci.* **2001**, *5*, 343−353.
(4) *Reactions and synthesis in surfactant systems*; Texter, J. Eds.; Surfactant Science Series 100; Marcel Dekker: New York, 2001.
(5) Chakrapani, M.; Rill, R. L.; Van Winkle, D. H. *Macromolecules* **2003**, *36*, 9050−9059.
(6) Strom, P. M.; Anderson, D. M. *Langmuir* **1992**, *8*, 691−709.
(7) Laversanne, R. *Macromolecules* **1992**, *25*, 489−491.
(8) Hentze, H. P.; Kaler, E. W. *Chem. Mater.* **2003**, *15*, 708−713.
(9) Antonietti, M.; Caruso, R. A.; Hentze, H. P.; Göltner, C. *Macromol. Symp.* **2000**, *152*, 163−172.
(10) Williams, R. J. J.; Rozenberg, B. A.; Pascault, J. P. *Adv. Polym. Sci.* **1997**, *128*, 95−156.
(11) Asnaghi, D.; Giglio, M.; Bossi, A.; Righetti, P. G. *J. Mol. Struct.* **1996**, *383* (1−3), 37−42.
(12) Kwok, A. Y.; Prime, E. L.; Qiao, G. G.; Solomon, D. H. *Polymer* **2003**, *44*, 7335−7344.
(13) Pacios, I. E.; Lindman, B.; Horta, A.; Thuresson, K.; Renamayor, C. S. *Colloid Polym. Sci.* **2002**, *280*, 517−525.
(14) Pacios, I. E.; Renamayor, C. S.; Horta, A.; Lindman, B.; Thuresson, K. *J. Phys. Chem. B.* **2002**, *106*, 5035−5041.
(15) Pacios, I. E.; Renamayor, C. S.; Horta, A.; Lindman, B.; Thuresson, K. *Macromolecules*, **2002**, *35*, 7553−7560.
(16) Pacios, I. E.; Renamayor, C. S.; Horta, A.; Lindman, B.; Thuresson, K. *Colloids Surf. A* **2003**, *218*, 11−20.
(17) Demé, B.; Dubois, M.; Zemb, T.; Cabane, B. *J. Phys. Chem.* **1996**, *100*, 3828−3838.
(18) Shea, K. J.; Stoddard, G. J.; Shavelle, D. M.; Wakui, F.; Choate, R. M. *Macromolecules* **1990**, *23*, 4497−4507.
(19) Ren, B.; Gao, F.; Tong, Z.; Yan, Y. *Chem. Phys. Lett.* **1999**, *307*, 55−61.
(20) Brinke, G.; Ikkala, O.; Ruokolanien; J.; Torkkeli, M.; Serimaa, R.; Vahvasellkä, S.; Saariaho, M. *Macromolecules* **1996**, *29*, 6621−6628.
(21) Dusek, K. *Mater. Sci. Technol.* **1997**, *18*, 401−427.
(22) Nallet, F.; Laversanne, R.; Roux, D. *J. Phys. II* **1993**, *3*, 487−502.
(23) Fontell, K. *J. Colloid Interface Sci.* **1973**, *44*, 318−329.
(24) Li, Y.-H.; Chan, L.-M.; Tyer, L.; Moody, R. T.; Himel, C. M.; Hercules, D. M. *J. Am. Chem. Soc.* **1975**, *97*, 3118−3126.
(25) Fontell, K. *J. Polym. Sci.* **1962**, *23*, 445−452.
(26) Flory, P. J. *Principles of Polymer Science*; Cornell University Press: New York, 1953; Chapter XIII.
(27) Kwok, A. Y.; Qiao, G. G.; Solomon, D. H. *Polymer* **2003**, *44*, 6195−6203.
(28) Asnaghi, D.; Giglio, M.; Bossi, A.; Righetti, P. G. *J. Chem. Phys.* **1995**, *103*, 9736−9742.
(29) Monleón Pradas, M.; Gómez Ribelles, J. L.; Serrano Aroca, A.; Gallego Ferrer, G.; Suay Antón, J.; Pissis, P. *Polymer* **2001**, *42*, 4667−4674.
(30) Alfrey, T.; Gurnee, E. F.; Lloyd, W. G. *J. Polym. Sci.* **1966**, *12*, 249−261.
(31) Peppas, N. A. *J. Bioact. Compat. Polym.* **1991**, *6*, 241−246.
(32) Brannon-Peppas, L.; Peppas, N. A. *Chem. Eng. Sci.* **1991**, *46*, 715−722.
(33) Trossarelli, L.; Meirone, M. *J. Polym. Sci.* **1962**, *57*, 445−452.
(34) Erman, B.; Mark, J. E. *Structure and Properties of Rubberlike networks*; Oxford University Press: New York, 1997.
(35) Bromberg, L.; Grosberg, A. Y.; Matsuo, E. S.; Suzuki, Y.; Tanaka, T. *J. Chem. Phys.* **1997**, *106*, 2906−2910.
(36) Molina, M. J.; Piérola, I. F.; Gómez-Antón, M. R. *Int. J. Polym. Mater.* **2002**, *51*, 477−484.

MA049758J